Arunchaitanya and Dey
AI in Civil Engineering (2023) 2:4
https://doi.org/10.1007/s43503-023-00013-3

ORIGINAL ARTICLE

Open Access

Sorptivity and rapid chloride ion penetration of self-compacting concrete using fly ash and copper slag

Sambangi Arunchaitanya[1] and Subhashish Dey[1*]

Abstract

This paper represents experimental work on the mechanical and durability parameters of self-compacting concrete (SCC) with copper slag (CS) and fly ash (FA). In the first phase of the experiment, certain SCC mixes are prepared with six percentages of FA replacing the cement ranging from 5% to 30%. In the second phase, copper slag replaces fine aggregate at an interval of 20% to 100% by taking the optimum percentage value of FA. The performance of SCC mixes containing FA and copper slag is measured with fresh properties, compressive, split tensile and flexural strengths. SCC durability metrics, such as resistance against chloride and voids in the concrete matrix, is measured with rapid chloride ion penetration test (RCPT) and sorptivity techniques. The microstructure of the SCC is analyzed by using SEM and various phases available in the concrete matrix identified with XRD analysis. It is found that when replacing cement with 20% of FA and replacing fine aggregate with 40% of copper slag in SCC, higher mechanical strengths will be delivered. Resistance of chloride and voids in the concrete matrix reaches the optimum value at 40%; and with the increase of dosage, the quality of SCC will be improved. Therefore, it is recommended that copper slag be used as a sustainable material for replacement of fine aggregate.

Keywords Copper slag, RCPT, Sorptivity, Self compacting concrete

1 Introduction

Concrete is a significant material for the infrastructure development in society. Self-compaction concrete (SCC) is a kind of concrete that settles and gets compacting by its gravity. A structure with high congested reinforcement is tough enough to compact the concrete in conventional methods. Therefore, SCC concrete is an alternative material that can flow and compact itself without any mechanical vibrations. Over the past few years, there has been an increasing interest in self-compaction concrete (Kumar & Bhattacharjee, 2003), which can provide more mechanical strength than regular concrete. The applications of SCC include bridge decks, dams, and tall structures (Oliveira et al., 2015). The properties of strength, workability and durability are considered as essential criteria of SCC. Many researchers are exploring the flowability, durability and strength performance of SCC. Durable concrete structures shall have proper and sufficient compaction (Palou et al., 2016). As a secondary product in coal burning, fly ash is widely used as a secondary cementitious material. There are two major types of ash: Class F and Class C, which can both improve such properties as sulphate resistance, freeze-thaw resistance, abrasion resistance and alkali-silica reaction of concrete. SCC is often substituted with mineral admixtures, including fly ash. High-quality powder content can be prepared by adding mineral additives, such as fly ash, nano copper slag, silica fume, etc. Fly ash is often used to reduce the viscosity of concrete and improve the rheological properties of final products (Praveen et al., 2019). Natural

*Correspondence:
Subhashish Dey
subhasdey633@gmail.com
[1] Civil Engineering Department, Gudlavaleru Engineering College, Gudlavalleru, Andhra Pradesh, India

aggregates are significant constituents in SCC, because they occupy 70% of the total volume of SCC. In addition, the primary purpose of using mineral admixtures is to minimize the demand of using natural aggregates and improve the durability and strength properties. It is costly to prepare artificial aggregates, and the naturally available aggregates have to be transported for a long distance to construction sites. Due to the rise of unauthorized sand mining, the demand for non-natural materials has become an issue in the construction industry. This is where alternate materials come into play, including copper slag (CS) material, which is an industrial residual waste and may be used in construction fields as an alternative material (Rossignolo, 2009).

Copper slag is obtained in the process of heating matte and refining copper. When yielding 1 ton of copper, about 2.2 to 3 tons of slag will be produced as a secondary product, which contains various oxides, like SiO_2, Al_2O_3, CaO, and Fe_3O_4. Globally, around 68.7 million tons of copper slag are produced, which is partially used as a replacement for sand in the construction industry. CS has lower water-absorbing capacity than natural river sand, but behaves with the same properties of river sand (Arunchaitanya & Arunakanthi, 2019; Geetha & Mahavan, 2017). By replacing fine aggregates with copper slag in concrete mixes, economical concrete production could be delivered. Technically, copper slag can improve the mechanical strength and quality of concrete. The CS replacement of aggregates has the advantage of decreased costs in disposing as well as diminished air pollution (Chand et al., 2016; Ishimaru et al., 2005). The existing research was mostly focused on the utilization of copper slag as fine aggregate in normal vibrated concrete. However, this study would, by using RCPT and sorptivity techniques, assess the durability of SCC after incorporating fly ash and copper slag as mineral admixtures.

Table 1 Chemical characteristics of OPC, fly ash (FA) and copper slag (CS)

Components	OPC	FA	CS
SiO_2	21.25	57.8	32.5
Al_2O_3	5.56	31.5	2.78
Fe_2O_3	4.12	4.5	55.82
CaO	60.52	1.15	4.6
MgO	2.15	0.25	1.56
SO_3	2.36	0.18	1.79
K_2O	0.65	0.96	0.71
Na_2O	0.42	0.63	1.24
TiO_2	0.23	1.52	0.24
Loss on ignition (%)	2.24	4.12	0
Sp. Gr	3.12	2.64	3.93

2 Materials and experimental procedure

In this study, cement was subjected to various tests, so as to establish its properties. The results of these tests are presented in Tables 1 and 2. Ultratech OPC was used in all the mixes; and fly ash was collected from locally available ready mix concrete. The characteristics are showcased in Tables 1 and 2.

2.1 Materials

To measure the workability of concrete pastes, a superplasticizer named CERA HYPER PLAST XR-W40 was used, which with had a specific gravity of 1.11 and a pH of 7. As a residual by-product that is produced during blending and refining copper, copper slag is a glassily structured material, with a very low absorbing capacity.

In order to pass the holes with the maximum size of 4.75 mm, the fine aggregate is taken; however, the crushed stones are coarse aggregates with a nominal size of 10–12 mm. Both the fine and coarse aggregates meet the specifications of IS:383–1970 Indian Standard. The physical characteristics of the coarse and fine aggregates are presented in Table 3.

2.2 Mix proportions

The SCC mixes are made with a total of 550 kg/m^3 of fine powder (cement + fly ash). This study is proposed to utilize the fine particle fly ash to partially replace the cement, while utilizing copper slag to partially replace the fine aggregates. The process was divided into two steps: First, FA was used as binding materials partially

Table 2 Physical characteristics of FA and cement

Physical properties	FA	Cement
Fineness Retained	15% (45 microns)	5% (90 microns)
Specific Gravity	2.64	3.12
Color	Grey	Dark grey
Normal Consistency	–	32%
Initial Setting	–	45 min
Final Setting	–	480 min

Table 3 Physical characteristics of the fine aggregate, coarse aggregate and copper slag

Properties	Fine aggregate	Coarse aggregate	Copper slag
Specific Gravity	2.64	2.72	3.93
Water Absorption (%)	0.95	0.1	0.1
Density kg/m^3	1580	1560	–
Fineness Modulus	2.55	6.69	3.61
Appearance	–	–	Black and glassy

in various percentages (5%, 10%, 15%, 20%, 25%, and 30%); second, the fine aggregates were also replaced with copper slag (20%, 40%, 60%, 80%, and 100%), taking 20% FA as a constant. The mix proportions are represented in Table 4.

2.2.1 Sample preparation

To determine the mix proportions, the materials were weighed individually. In the rotating pan, the materials were mixed for about 5 min. The fresh properties were determined for the flowability of concrete paste. Figures 1 and 2 show the sample remolded after 24 h of water

Table 4 Details of SCC mixes

Mix ID	OPC (kg/m^3)	FA (kg/m^3)	CS (kg/m^3)	River sand (kg/m^3)	Crushed stone (kg/m^3)	SP (kg/m^3)	Water (kg/m^3)
FA0	550	0	–	924.52	779.35	2.2	165
FA5	522.5	27.5	–	924.52	779.35	2.09	165
FA10	495	55	–	924.52	779.35	1.98	165
FA15	467.5	82.5	–	924.52	779.35	1.87	165
FA20	440	110	–	924.52	779.35	1.76	165
FA25	412.5	137.5	–	924.52	779.35	1.65	165
FA30	385	165	–	924.52	779.35	1.54	165
FA20 + CS20	440	110	184.9	739.61	779.35	1.76	165
FA20 + CS40	440	110	369.80	544.7	779.35	1.76	165
FA20 + CS60	440	110	544.7	369.80	779.35	1.76	165
FA20 + CS80	440	110	739.61	184.9	779.35	1.76	165
FA20 + CS100	440	110	**924.52**	**0**	**779.35**	**1.76**	**165**

Fig. 1 Slump flow tests and placements of concrete in the specimen

Fig. 2 Slump flow and L-box

curing and testing at the required age of room temperature. The cubes with a size of 150 mm × 150 mm × 150 mm were used to measure the compressive strength; those of 150 mm × 300 mm cylinders were to measure the split tensile; those of 100 mm × 100 mm × 500 mm beams were to measure the flexural strength; and those of 100 mm × 50 mm cylindrical shaped specimens were to measure RCPT. All the test readings were taken from the average of three sample readings.

3 Tests on specimen

3.1 SCC Properties

To determine the self-compacting properties, such as the slump flow, the tests of T_{50} cm time, L-box, V-funnel flow and U-box were performed. SCC's filling ability was evaluated in U-box test, while the flowing ability was examined in slump flow test. Fresh concrete was layered in slump cone and pulled upwards; and the spreading of concrete paste in two right-angled directions of the table was measured. A slump flow ranges from 650 mm to 800 mm, which is a considerable limit for self-compacting concrete (Johnsirani et al., 2013). L-box ranges from 0.8 mm to 1.0 mm, U-box ranges from 0 mm to 30 mm, V-funnel test flow time is below 6 s, and T_{50} cm test for less than 5 s is suggested for the concrete, so as to satisfy the standard for SCC as specified in EFNARC.

3.2 Mechanical properties

The tests of compressive strength, split tensile strength and flexural strength were used to evaluate the mechanical properties of SCC at specified ages of 7 days, 28 days, 56 days and 90 days. Specimen sizes were explained in sample preparation. These tests were conducted on a compressive testing machine called 2000 kN.

3.3 Rapid chloride ion permeability test

A rapid chloride ion penetration test (RCPT) was implemented to estimate the permeability of chloride ions into the matrix as per the code of ASTM C 1202. In the test, a 100 × 50 mm cylindrical specimen was used. A potential difference of 60 VDC was perpetuated throughout the specimen was tested. In this process, two solutions were used: a sodium chloride solution (NaCl) on one side, and a sodium hydroxide solution (NaOH) on the other, as shown in Fig. 10. The charges flowing through in a total time of 6 h were measured. Nowadays, certain concrete buildings are constructed according to the requirements for low-permeability concrete. RCPT is widely accepted in the construction industry as a means of measuring chloride permeability.

3.4 Water sorptivity

As another measure of durability, sorptivity was calculated by observing the rate at which the mass of an immersed concrete specimen rose as a function of time, with emphases on the onset of absorption as well as on the subsequent absorption. The initial absorption lasted for a time period between 1 min and 6 h of immersion, while the secondary absorption lasted for a time period between 6 h and 7 days of immersion, followed by necessary cure times. The total absorption values for both the primary and secondary absorptions were averaged for further analysis. After being dried in an oven and cooled to the room temperature, a 150 mm cube was submerged in water to the depth of 10 mm. Except for the bottom surface, all sides of the specimen were wrapped in polythene or waterproof plaster to prevent water molecules from evaporating or being lost. Absorption mass was measured by weighing the concrete cube at certain intervals in accordance with ASTM C1585.

3.5 Microstructure

As specified in ASTM C1723, a scanning electron microscope (JOEL IT200, Japan) was utilized to analyze the manufacturing of cement wet goods and the mechanisms driving strength augmentation. The phases present in the concrete matrix were determined by using a powdered diffractometer (PANalytical, United Kingdom). ASTM C1365 allows for the detection of various phases involved in the development of strength. Following the compression test in the CTM, samples were collected for SEM and XRD analysis. The obtained samples were ground to a fineness of 95 percent of particles being less than 10μ and no more than 5 percent of particles being 1μ in the preparation for the QXRD analysis. In the experiment, ethylene glycol was fed to the samples in a tungsten carbide ring-and-puck mill, as specified in ASTM C1723. SEM examination samples were prepared according to the methodology under ASTM C1723. To begin with, the samples were examined for efflorescence, carbonation, and other potential problems. Secondly, the samples were dried in a 105 °C oven before cleaned and seasoned to reduce their sizes with ethanol alcohol. Finally, polishing was performed to prepare the samples for microstructural and quantitative microanalyses.

4 Results and discussion

4.1 Properties of fresh concrete

The outcomes of fresh SCC characters, such as Slump flow, U-box, V-funnel and L-box, are presented in Table 5. In the process of slump flow, all SCCs exhibited a comfortable flow in a range of 650 mm–800 mm, indicating a good sign (Safi et al., 2013). FA improved the slump

Table 5 Characteristics of Fresh SCC

Mixes	Slump (mm)	T_{50} (sec)	L-box (ratio)	U-box (mm)	V-funnel (sec)
F0	680	4.28	0.8	28	9.35
F5	685	4.25	0.805	28	9.26
F10	692	4.11	0.81	27	9.02
F15	705	3.98	0.82	26	8.64
F20	718	3.71	0.83	25	8.23
F25	732	3.42	0.84	23	8.11
F30	750	3.19	0.85	21	7.56
F20 + CS20	726	3.4	0.84	23	7.79
F20 + CS40	746	3.05	0.86	22	6.97
F20 + CS60	764	2.61	0.88	19	6.16
F20 + CS80	772	2.49	0.92	14	5.73
F20 + CS100	786	2.30	0.96	10	5.16

flow parameters from 680 mm to 750 mm. After incorporating CS, the flowability was further enhanced from 718 mm to 780 mm. Similarly, the V-funnel test process had a flowing time ranging from 6 secs to 12 secs, as per the European guidelines. FA reduced the time taken to flow through V-funnel by almost 2 s, while CS reduced it by two more secs. Coarse aggregate size was limited to 16 mm, thus helping avoid the blocking of aggregates in congested reinforcement. In the L-box test, rebars were arranged in a 20 mm space. The ratio of L-box with a depth ratio for the SCC mixes should be above 0.8.

Supplementary cementitious materials (FA) improved the passing ability, which was scaled to 0.85 at 30% substitution; the increase of spherical shaped particles enhanced the ball bearing effect (Uysal & Sumer, 2011). CS improved the scale to 0.96 at 100% fine aggregate replacement. The difference of U-box in the heights of H_2-H_1, i.e., concrete in the two compartments, should be in the range of 0 mm–30 mm, as shown in Figs. 2 and 3. By adding both mineral admixtures, the filling ability was improved from 28 mm to 10 mm. The T_{50} slump flowing time of the mix should be more than 2 s. In combination, FA and CS enhanced the flowability as per the EFNARC Standard guidelines. With the rise of CS particles in the fresh concrete, the passing ability and filling ability of SCC were enhanced, due to the low absorption character of CS.

4.2 Compressive strength

The test for the compressive strength of SCC was conducted on cubes of a 150 mm × 150 mm × 150 mm size after fresh properties of each mix variant were acquired. The replacement of cement with fly ash was tried in various percentages: 0%, 5%, 10%, 15%, 20%, 25% and 30%. The values of compressive strength of the nominal mix were 55.78 Mpa, 68.5 Mpa, 73.05 Mpa, and 74.5 Mpa for 7, 28, 56, 90 days for age of curing. The maximum compression strength was obtained at 20% of fly ash replacement, with an increase by 12%, 13.14%, 17.27% and 18.59% for 7, 28, 56 and 90 days, as shown in Fig. 4. Scanning Electron Microscope was used to analyze the microstructure of SCC. As seen in Fig. 4, the SEM images of ettringite were formed in the concrete matrix. Cracks and voids available in the specimen were observed. The enhanced ettringite was developed, responsible for the strength increment. In the pictures, the spherical-shaped fly ash particles can be observed, which are the unreacted fly ash particles (Zhao et al., 2012). Cracks and pores or voids are reduced in the FA-added concrete matrix, which is denser than the conventional SCC mix (F0), possibly due to pozzolanic action of FA (Bouzoubaa & Lachemi, 2001).

Various percentages of copper slag were tried in SCC: 20%, 40%, 60%, 80% and 100%. The highest strengths were obtained at 40% copper slag replacement, with an increase of 6.52%, 10.7%, 6.16% and 8.87% to the FA20 mix for 7, 28, 56 and 90 days of curing ages, as shown in

Fig. 3 V-funnel and U-box

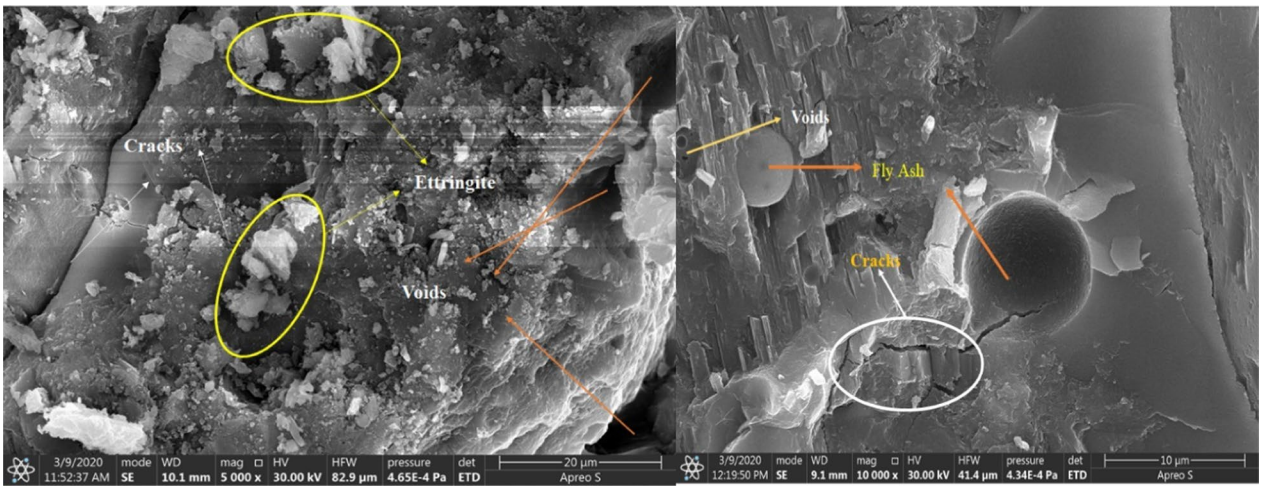

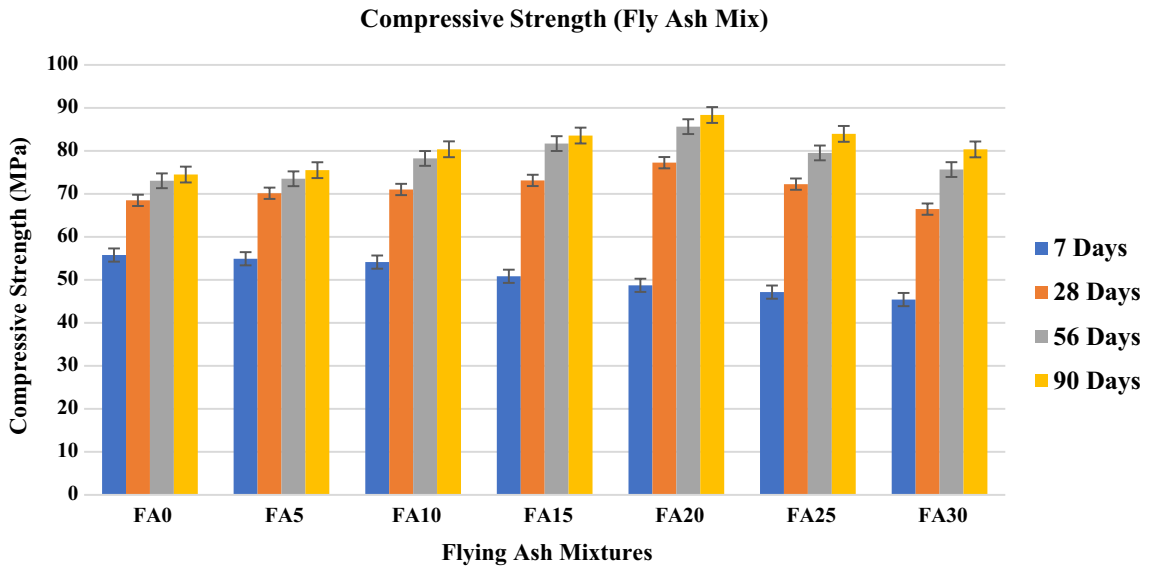

Fig. 4 Compressive strength of fly ash SCC mixes and SEM images of F0 and F20

Fig. 5. With the replacement of river sand with CS, the enhanced ettringite was observed in the SEM image of F20 + CS40 mix sample. The formation of ettringite facilitated the development of strength in the concrete matrix. Discussions in Sect. 4.1 established that the addition of copper slag and fly ash enhanced the fresh concrete's characteristics. SCC with fly ash and copper slag resulted in a transition from SF2 to SF3 slump flow. Thanks to its great fluidity property, SCC can be utilized for highly conjusted reinforced structural members. Void reduction in the concrete matrix is driven by this process. The majority of the voids were minimized with the usage of CS. The smaller particle size was adjusted to the pores and helped enhance the compressive strength. Due to the hydration process, C-S-H and secondary C-S-H were formed in the concrete matrix (Xotta et al., 2015).

4.3 Split tensile strength

The tensile strength of the concrete was evaluated on 100 mm dia and 300 mm long cylinders. The substitution of cement with the fly ash was tried in various intervals: 0, 5%, 10%, 15%, 20%, 25% and 30%. The nominal mix strength values were 3.83 Mpa, 3.9 Mpa, 4.21 Mpa, and 4.56 Mpa for 7, 28, 56 and 90 days, as shown in Fig. 6. The maximum stability was obtained in the 20% replacement, with an increase of 20.76%, 7.69%, 7.6% and 10.74% on the 7th, 28th, 56th and 90th day, respectively. Due to the pozzolanic activity of FA, this may have happened. The reactive silica in FA reacted with the portlandite,

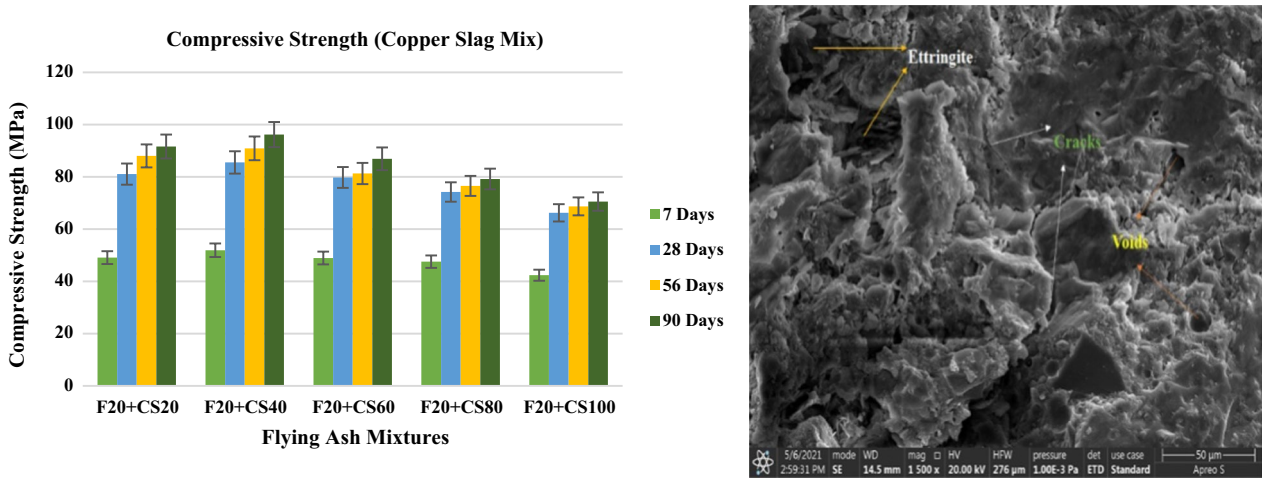

Fig. 5 Compressive strength of copper slag SCC mixes and SEM images of F20 + CS40

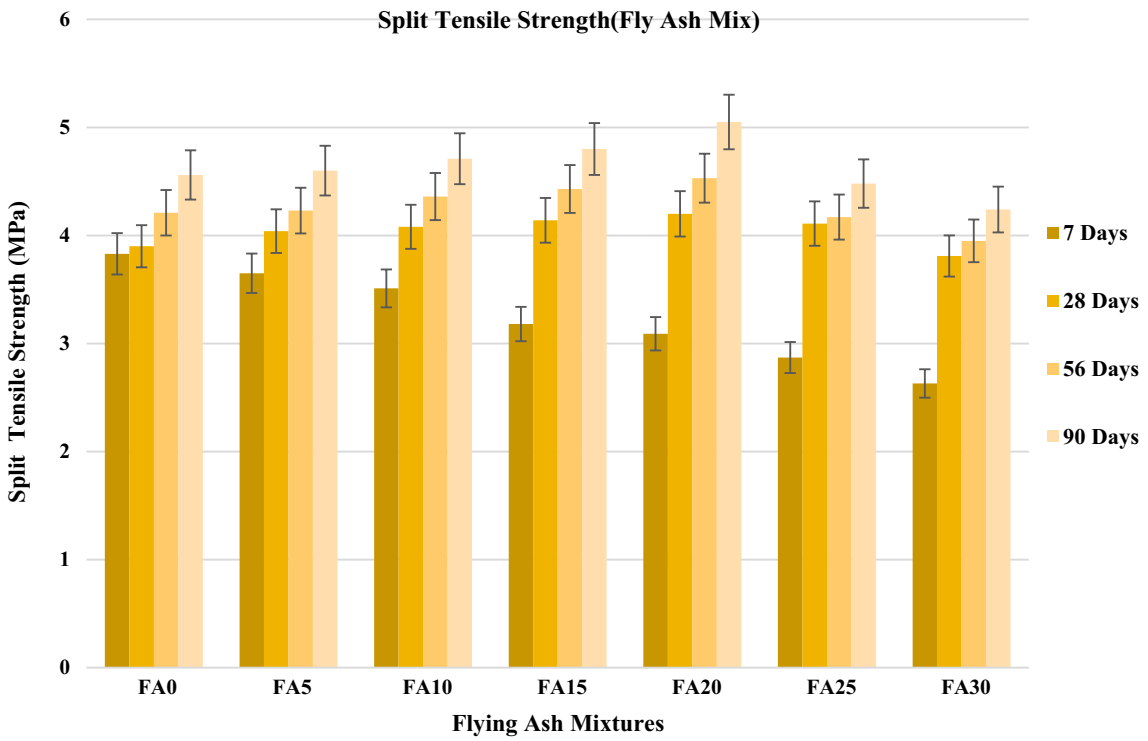

Fig. 6 Split tensile strength of fly ash SCC mixes

forming the secondary C-S-H. With the improvement of the strength of the concrete, the split tensile may also be enhanced (Zhutoysky & Kovler, 2012).

River sand was replaced with the copper slag in specific percentages: 20%, 40%, 60%, 80% and 100%. The highest split tensile strength was obtained at 40% copper slag replacement, with an increase of 3.13%, 14.76%, 18.10% and 13.46% to the FA20 mix on the 7th, 28th, 56th and 90th day in the period (age) for curing, respectively, as shown in Fig. 7. CS in SCC augmented the homogeneity of the concrete. Segregation and bleeding of concrete were reduced with CS. Enhanced homogeneity increased the split tensile strength of SCC (Krishnudu et al., 2020).

River sand was replaced with the copper slag in specific percentages: 20%, 40%, 60%, 80% and 100%. The highest split tensile strength was obtained at 40%

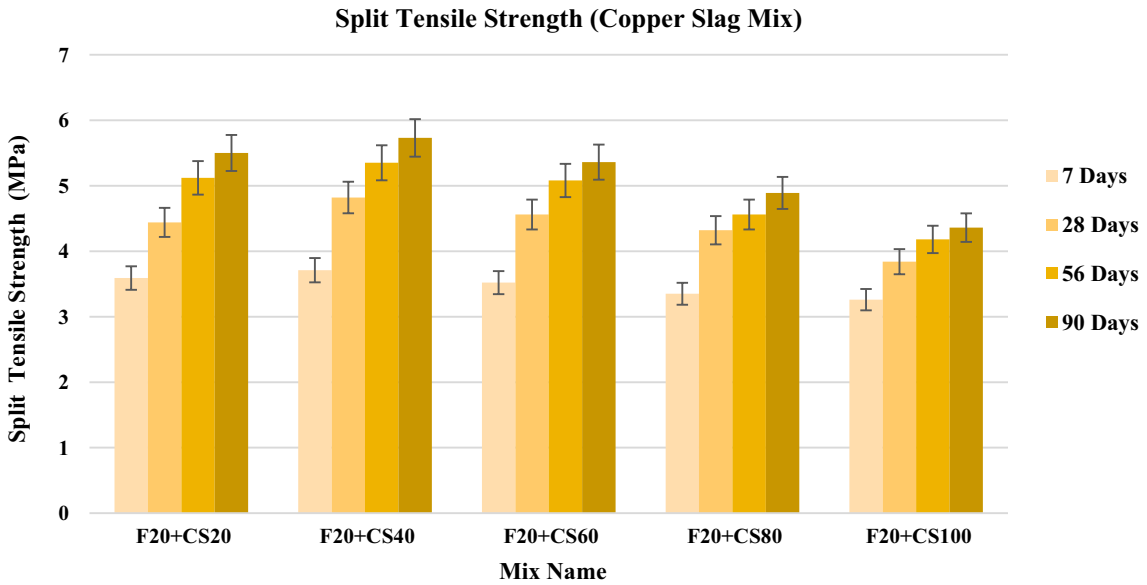

Fig. 7 Split Tensile Strength of Copper Slag SCC Mixes

copper slag replacement, with an increase of 3.13%, 14.76%, 18.10% and 13.46% to the FA20 mix on the 7th, 28th, 56th and 90th day of the period (age) curing, respectively, as shown in Fig. 7. CS in the SCC augmented the homogeneity of the concrete. Segregation and bleeding of the concrete was reduced with CS. Enhanced homogeneity boosted the split tensile strength of SCC (Wang et al., 2020). All the cylinders showcased a good ductile behavior. The splitting tensile strength was enhanced with the age of curing. The difference in strength between concrete specimens became highly distinct in the beginning of curing itself (Dey et al., 2022).

4.4 Flexural strength

This test was conducted on a beam of 500 mm × 100 mm × 100 mm size. The substitution of cement with fly ash was tried in various percentages: 0%, 5%, 10%, 15%, 20%, 25% and 30%. The conventional mix strength values are 8.31 MPa, 9.04 MPa and 9.12 MPa for

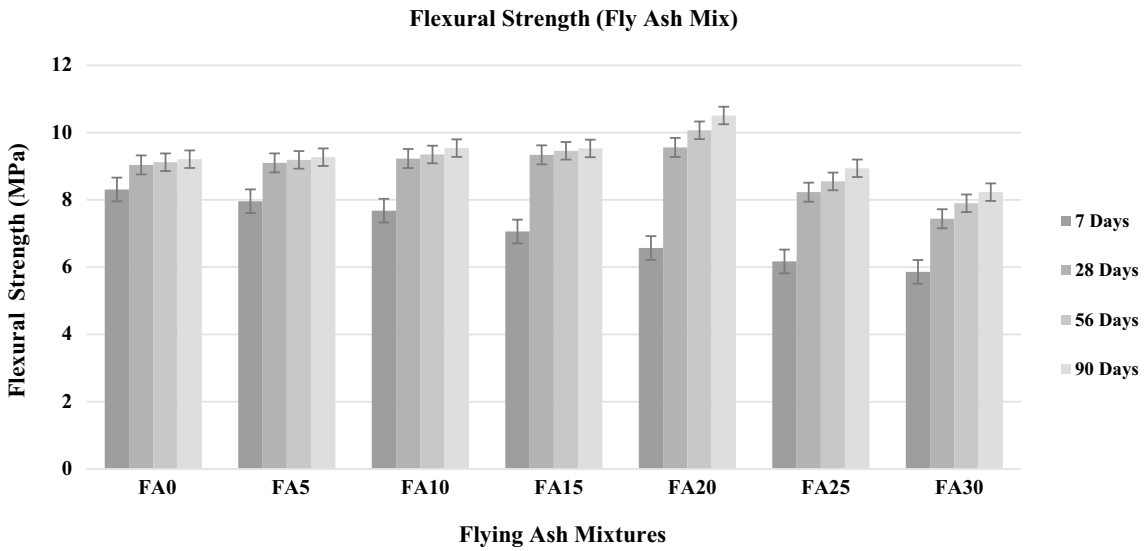

Fig. 8 Flexural strength of fly ash SCC mixes

the periods of 7, 28, 56 and 90 days of curing age. The maximum strength was obtained at 20% replacement, with an increase of 20.93%, 5.75%, 10.41% and 14.11% for the ages of 7, 28, 56 and 90 days, as shown in Fig. 8. The replacements of sand with the copper slag (CS) in different percentages were 20%, 40%, 60%, 80% and 100%. The highest flexural strength for copper slag replacement was obtained at 40%, with an increase of 10.98%, 15.37%, 12.11%, and 9.89% to the FA20 mix on the 7th, 28th, 56th and 90th day, respectively, as shown in Fig. 9 (Rojas et al., 2020).

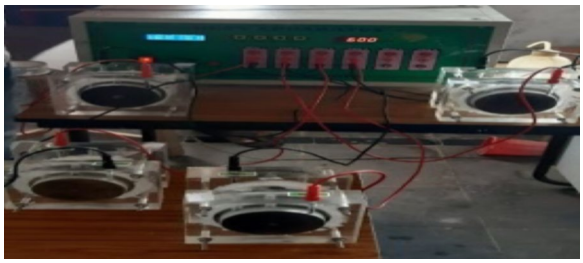

Fig. 10 Rapid chloride penetration test

4.5 Rapid chloride ion penetration test

Resistances against chloride ion penetration in all the SCC mixes were at a low or very low level. Fly ash mixes were standing between 700 Coulombs and 1,600 Coulombs on the 28th and 56th day. The result of the coulomb charge in the conventional mix was 1,597.32 Coulombs at the 56th day, indicating a high penetrability. The coulomb charge of the 20% mix was 726.42 Coulombs on the 56th day, so the penetration was very low, as indicated in Figs. 10 and 11. The SCC mixes with copper slag showed 1000 Coulomb to 500 Coulombs for 28 and 56 days. The copper slag resulted in a coulomb charge of 100%; the mix was standing at 889.41 Coulombs, with very low penetration; and the optimum strength-based replacement of 40% CS had 552.17 Coulombs, with the least penetration at the 56th day for age, as presented in Fig. 12.

Ananthi et al.(2017) have found that the addition of fly ash will deliver a low penetrability from approximately 3000 Coulombs to below 1000 Coulombs. In addition to developing a dense C-S-H, the workability can also help enhance the homoginity of concrete. As discussed in Sect. 4.1, the increase of copper slag and fly ash improved the fresh properties, showing that SCC with fly ash and copper slag changed the slump flow from SF2 to SF3. This indicates that SCC can be used for highly conjusted reinforcement, because it has a high fluidity property and can help reduce the voids in concrete matrixes (Dey et al., 2021).

4.6 XRD analysis

XRD experiments were implemented to determine how the concrete matrix would change over the course of water curing. Adding copper slag to SCC did not cause any significant phase changes. After a compressive strength test on cubes in CTM, certain samples were acquired. Powdered bits were used in two angles, ranging from 10 to 90 degrees apart (Madduru et al., 2020). Figure 13 showed that the XRD patterns of the mixes of F0, F20 and F20 + CS40. The conventional SCC mix has a maximum peak of 18, with an intensity of 27.6 at 27 nm, and the phases are portlandite and quartz. XRD analysis shows that the ettringite development could enhance the compressive strength as SCC age was increased. The non-blended SCC mix, with an intensity of 61.4 at

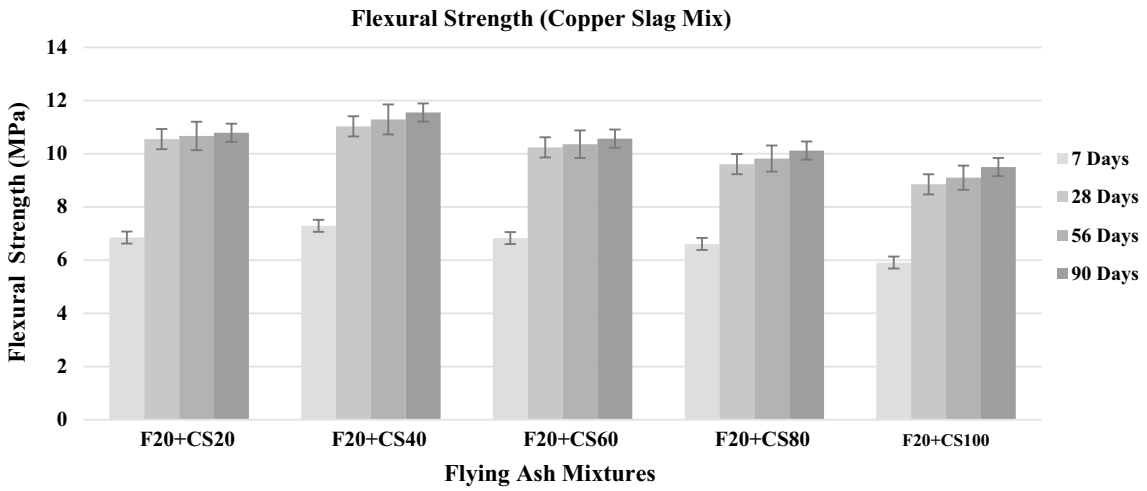

Fig. 9 flexural strength of copper slag SCC mixes

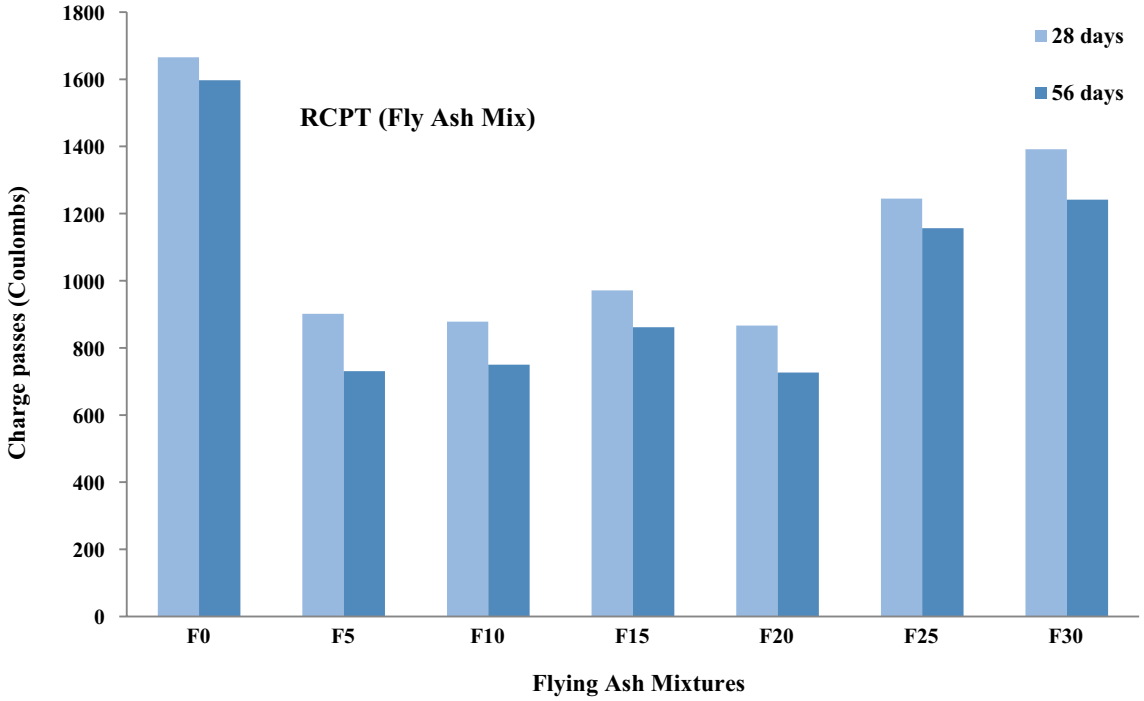

Fig. 11 Charges passed with different percentages of fly ash SCC

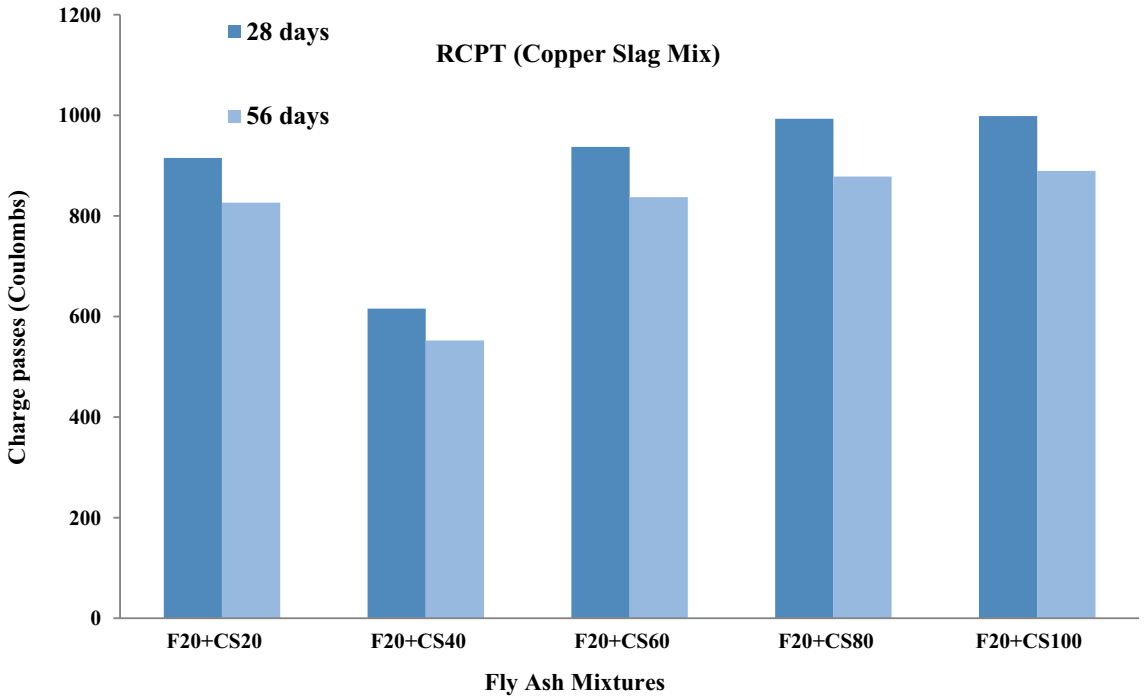

Fig. 12 Charges passed with different percentages of copper slag in SCC

26.55 nm, had a lower maximum possible peak intensity than that of this mix. Ettringite, Quartz, and Calcium hydroxide were all present in the F20 + CS40 ID sample. CS increased from 0 to 40% in river sand, resulting in an increase of 68.16 in Quartz phase intensity at 27.38 nm. The results of both SEM and XRD indicate the presence

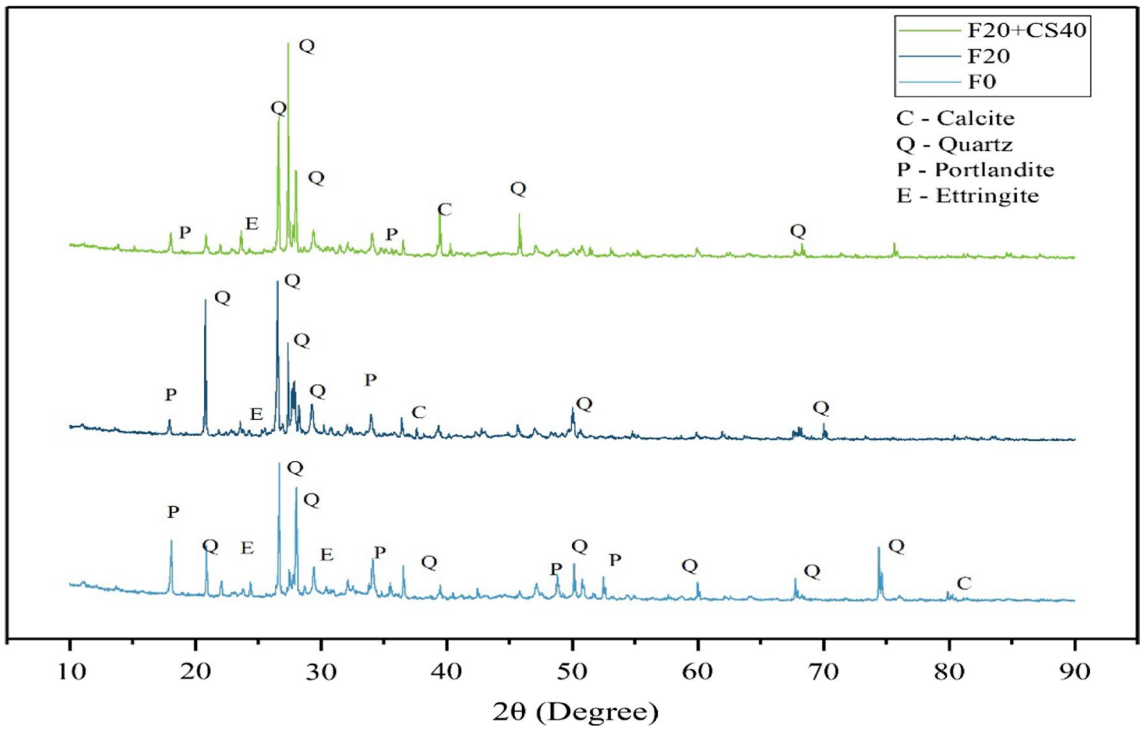

Fig. 13 XRD analysis of SCC

of these ettringite residues (Praveen Kumar & Dey, 2023). Both CF20 and CF20CS40 produced ettringite when calcium reacted with cement sulphates and aluminates to form ettringite. Secondary C-S-H was created when portlandite reacted with reactive silica in FA; the ratio of calcium to silica determined how much secondary C-S-H would be formed. The samples had a similar diffraction pattern and did not differ significantly from the control sample in terms of amorphous and crystalline degrees (Dinakar et al., 2013).

4.7 Sorptivity

Sorptivity of SCC concrete is related to the capillary pores in concrete. A high number of pores indicate a higher sorptivity and a bigger chance to become poor concrete. It was found that the sorptivity coefficient would decrease with the consolidation of FA and CS, as compared to the control mix. Sorptivity was used to calculate the amount of water absorbed by hydraulic concrete (Shafeeque et al., 2016). Sorptivity was measured in the initial and secondary absorption tests. In the initial absorption, the experiment completed in 6 h of test, as shown in Figs. 14 and 15.

And the secondary absorption lasted for up to 7 days of processing, as shown in Figs. 16 and 17. The linear coefficient indicated the quality of the concrete. A large amount of water was absorbed through micropores, and the incorporation of fly ash and copper slag led to less absorption of water. The effect of pH on the carbonation level is determined by the colour (Kadhum, 2014). The density of construction materials that have been hardened is determined by the unit weight of constituent materials and the volume of void space.

As discussed earlier, the sorptivity of the concrete is directly proportional to the volume of voids available in the concrete matrix. Fresh properties play an influential role in achieving a low volume of voids. As the filling ability increased for SCC, the filling of concrete is even higher in the framework. However, the voids can be reduced by the increase of homogeneity. The reduction of voids would adversely affect the capillary action of concrete. Capillary action would be decreased if there is a reduction in the sorptivity of SCC (Prabhu et al., 2018).

5 Conclusions

From the present experimental investigation, the following conclusion can be drawn. The fresh properties of SCC mixes are within the scope of EFNARC guidelines, and the fly ash replacement in around 20%–30% and proper copper slag addition would deliver superior performance for SCC. Strength would increase with the decreasing of w/c and can deliver a good strength at w/c of 0.3 at 550 kg/m^3. The optimum percentage of fly ash

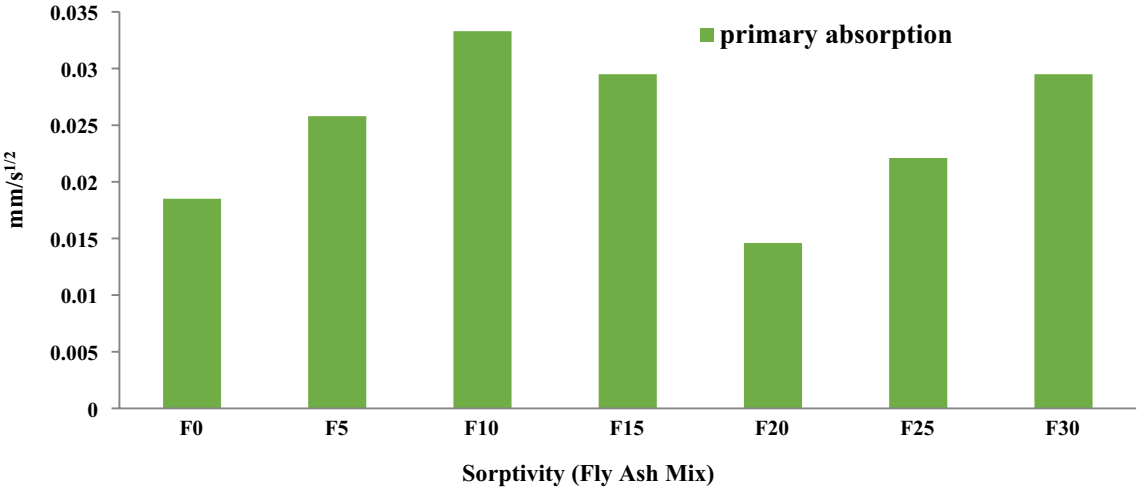

Fig. 14 Primary absorption of sorptivity for fly ash SCC mixes

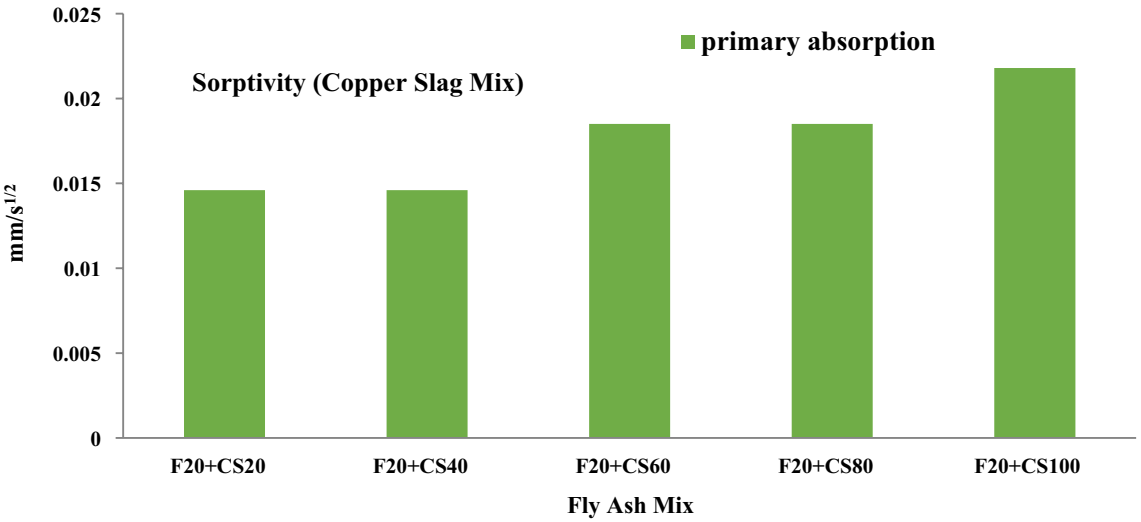

Fig. 15 Primary absorption of sorpitivity for copper slag SCC

and copper slag is 20% and 40%, respectively. The optimum results were achieved in the tests. In SCC mixes, for compressive strength results of fly ash replacement, the maximum strength results are 55.78 Mpa, 68.5 Mpa, 73.05 Mpa and 74.5 Mpa on the 7th, 28th, 56th, and 90th day, respectively. Copper slag replacement delivered the maximum strength of 51.23Mpa, 85.53, 90.92, and 96.19 Mpa on the 7th, 28th, 56th, and 90th day, respectively. As to the SCC mixes' strength results for split tensile of fly ash replacement, the maximum strength results were 3.83, 3.9, 4.21, and 4.56 MPa on the 7th, 28th, 56th, and 90th day, respectively. Copper slag replacement delivered the maximum strength of 3.71, 4.82, 5.35, and 5.73 MPa on the 7th, 28th, 56th, and 90th day, respectively. As to SCC mixes' flexural strength results of fly ash replacement, the maximum strength of 8.31, 9.04, 9.12 and 9.21 Mpa were delivered on 7th, 28th, 56th and 90th day, respectively. Copper slag replacement's maximum strength was 7.29, 11.03, 11.29, and 11.55 MPa on the 7th, 28th, 56th and 90th day, respectively. SCC mixes manufactured with FA could reduce the chloride ion penetration within the

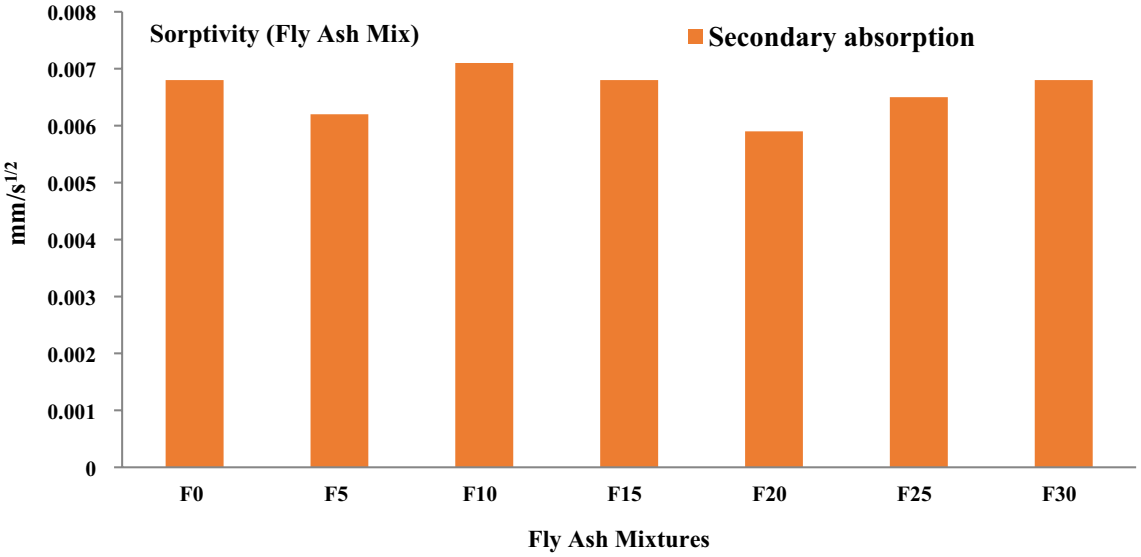

Fig. 16 Secondary absorption of sorptivity for fly ash SCC mixes

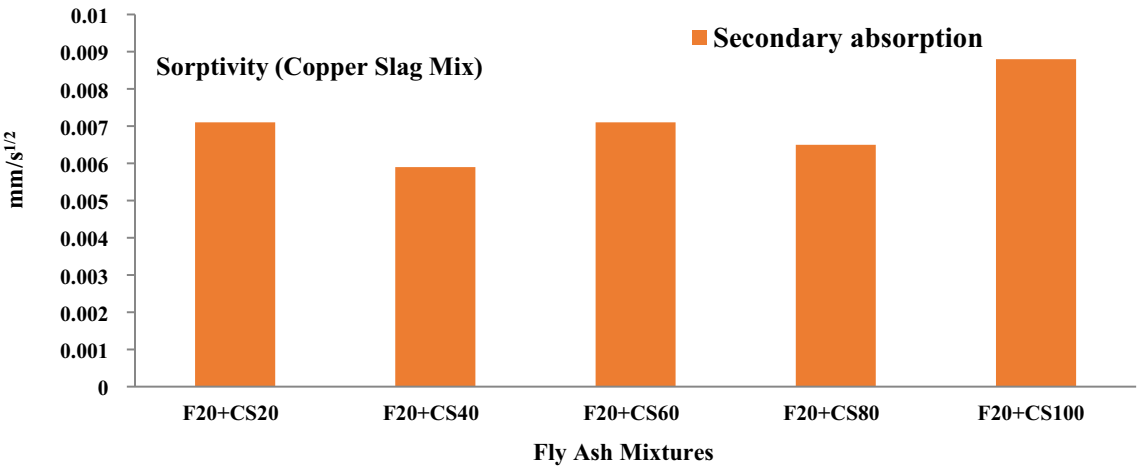

Fig. 17 Secondary absorption of sorptivity for copper slag SCC mixes

range of 700 to 1600 Coulombs on the 28th and 56th day. Copper slag mixes ranged from 500 to 1000 Coulombs at a very low level on the 28th and 56th day. The sorptivity coefficient would decrease with FA and CS as compared to the control mix.

Acknowledgements
The authors are thankful for the support from all the faculty members and lab in charges of Civil Engineering Department, Gudlavalleru Engineering College.

Author contributions
Both authors read and approved the final manuscript.

Funding
This research did not receive any specific grant from any public, private, or non-profit funding agency.

Availability of data and materials
The statements in the paper are properly cited in the manuscript and no additional data is available.

Declarations

Competing interests
The authors declare no conflict of interest.

Received: 25 January 2023 Revised: 5 May 2023 Accepted: 10 May 2023
Published online: 06 June 2023

References

Ananthi, A., Ranjith, R., Latha, S. S., & Raj, R. V. (2017). Experimental study on the properties of self-curing concrete. *International Journal of Concrete Technology, 3*(1), 8–13.

Arunchaitanya, S., & Arunakanthi, E. (2019). Usage of mineral admixtures in self compacting concrete—A review. *International Journal of Innovative Technology and Exploring Engineering, 8*(3), 2.

Bouzoubaa, N., & Lachemi, M. (2001). Self-compacting concrete incorporating high volumes of class F fly ash: Preliminary results. *Cement and Concrete Research, 31*(3), 413–420. https://doi.org/10.1016/S0008-8846(00)00504-4

Chand, M. S. R., Kumar, P. R., Giri, P. S. N. R., Kumar, G. R., & Rao, M. V. K. (2016). Influence of paraffin wax as a self-curing compound in self-compacting concretes. *Advances in Cement Research, 28*(2), 110–112. https://doi.org/10.1680/jadcr.15.00062

Dey, S., Kumar, V. V. P., Goud, K. R., & Basha, S. K. J. (2021). State of art review on self compacting concrete using mineral admixtures. *Journal of Building Pathology and Rehabilitation, 6*(18), 1–23. https://doi.org/10.1007/s41024-021-00110-9

Dey, S., Praveen, V. V. K., & Akula, V. P. M. (2022). An experimental study on strength and durability characteristics of self-curing self-compacting concrete. *Structural Concrete*. https://doi.org/10.1002/suco.202100446

Dinakar, P., Kartik Reddy, M., & Sharma, M. (2013). Behaviour of self-compacting concrete using Portland pozzolana cement with different levels of fly ash. *Materials and Design, 46*, 609–616. https://doi.org/10.1016/j.matdes.2012.11.015

Geetha, S., & Madhavan, S. (2017). High performance concrete with copper slag for marine environment. *Materials Today Proceedings, 4*(2), 3525–3533. https://doi.org/10.1016/j.matpr.2017.02.243

Ishimaru, K., Mizuguchi, H., Hashimoto, C., Ueda, T., Fujita, F., & Ohmi, M. (2005). Properties of concrete using copper slag and second class fly ash as a part of fine aggregate. *Zair. Soc. Mater. Sci. Japan, 54*(8), 828–833. https://doi.org/10.2472/jsms.54.828

Johnsirani, K.S., Jagannathan, A. and Kumar, R.D. (2013). Experimental investigation on self-compacting concrete using quarry dust. *International Journal of Scientific and Research Publications 3*, 1–5. https://www.ijsrp.org/research-paper-0613/ijsrp-p18127.pdf

Kadhum, M. M. (2014). Effect of metakaolin and fly ash on properties of self compacting concrete through accelerated curing. *International Journal of Scientific & Engineering Research, 5*(12), 11.

Krishnudu, D. M., Sreeramulu, D., & Reddy, P. V. (2020). A study of filler content influence on dynamic mechanical and thermal characteristics of coir and luffa cylindrica reinforced hybrid composites. *Construction and Building Materials, 251*, 119040. https://doi.org/10.1016/j.conbuildmat.2020.119040

Kumar, R., & Bhattacharjee, B. (2003). Porosity, pore size distribution and in situ strength of concrete. *Cement and Concrete Research, 33*(1), 155–164. https://doi.org/10.1016/S0008-8846(02)00942-0

Madduru, S. R. C., Shaik, K. S., Velivela, R., & Karri, V. K. (2020). Hydrophilic and hydrophobic chemicals as self curing agents in self compacting concrete. *Journal of Building Engineering, 28*, 101008. https://doi.org/10.1016/j.jobe.2019.101008

Oliveira, M. J., Ribeiro, A. B., & Branco, F. G. (2015). Curing effect in the shrinkage of a lower strength self-compacting concrete. *Construction and Building Materials, 93*, 1206–1215. https://doi.org/10.1016/j.conbuildmat.2015.04.035

Palou, M. T., Kuzielová, E., Žemlička, M., Boháč, M., & Novotný, R. (2016). The effect of curing temperature on the hydration of binary Portland cement. *Journal of Thermal Analysis and Calorimetry, 125*(3), 1301–1310. https://doi.org/10.1007/s10973-016-5395-9

Prabhu, P.S., Nishaant, H. and Anand, T. (2018). Behavior of self-compacting concrete with cement replacement materials. *International Journal of Chemical, Environmental & Biological Sciences 2*(3), 151–156. https://www.ijitee.org/wp-content/uploads/papers/v8i2s/BS2666128218.pdf

Praveen, K. V. V., Prasad, N., & Dey, S. (2019). Influence of metakaolin on strength and durability characteristics of ground granulated blast furnace slag based geopolymer concrete. *Structural Concrete*. https://doi.org/10.1002/suco.201900415

Praveen Kumar, V. V., & Dey, S. (2023). Study on strength and durability characteristics of nano-silica based blended concrete. *Hybrid Advances, 2*, 100011. https://doi.org/10.1016/j.hybadv.2022.100011

Rojas, D. P. H., Pineda-Gomez, P., & Guapacha-Flores, J. F. (2020). Effect of silica nanoparticles on the mechanical and physical properties of fibercement boards. *Journal of Building Engineering, 31*, 101332. https://doi.org/10.1016/j.jobe.2020.101332

Rossignolo, J. A. (2009). Interfacial interactions in concretes with silica fume and SBR latex. *Construction and Building Materials, 23*(2), 817–821. https://doi.org/10.1016/j.conbuildmat.2008.03.005

Safi, B., Ghernouti, Y., Rabehi, B., & Aboutaleb, D. (2013). Effect of the heat curing on strength development of self-compacting mortars containing calcined silt of dams and ground brick waste. *Materials Research, 16*(5), 1058–1064. https://doi.org/10.1590/S1516-14392013005000094

Shafeeque, V.M., Sanofar, P.B., Praveen, K.P., Nikhil, V.P. and Krishna, P.M.G. (2016). Strength comparison of self curing concrete and normal curing concrete. *International Journal of Civil Engineering 3*(3), *47–52*. https://www.internationaljournalssrg.org/IJCE/2016/Volume3-Issue3/IJCE-V3I3P110.pdf

Uysal, M., & Sumer, M. (2011). Performance of self-compacting concrete containing different mineral admixtures. *Construction and Building Materials, 25*(11), 4112–4120. https://doi.org/10.1016/j.conbuildmat.2011.04.032

Wang, Y., Liu, F., Yu, J., Dong, F., & Ye, J. (2020). Effect of polyethylene fiber content on physical and mechanical properties of engineered cementitious composites. *Construction and Building Materials, 251*, 118917. https://doi.org/10.1016/j.conbuildmat.2020.118917

Xotta, G., Mazzucco, G., Salomoni, V. A., Majorana, C. E., & Willam, K. J. (2015). Composite behavior of concrete materials under high temperatures. *International Journal of Solids and Structures, 64*(10), 86–99. https://doi.org/10.1016/j.ijsolstr.2015.03.016

Zhao, H., Sun, W., Wu, X., & Gao, B. (2012). Effect of initial water-curing period and curing condition on the properties of self-compacting concrete. *Materials and Design, 35*, 194–200. https://doi.org/10.1016/j.matdes.2011.09.053

Zhutovsky, S., & Kovler, K. (2012). Effect of internal curing on durability-related properties of high performance concrete. *Cement and Concrete Research, 42*(1), 20–26. https://doi.org/10.1016/j.cemconres.2011.07.012

Publisher's Note